Nonredox thiolation in tRNA occurring via sulfur activation by a [4Fe-4S] cluster

Simon Arragain, Ornella Bimai, Pierre Legrand, Sylvain Caillat, Jean-Luc Ravanat, Nadia Touati, Laurent Binet, Mohamed Atta, Marc Fontecave, Béatrice Golinelli-Pimpaneau

▶ **To cite this version:**

Simon Arragain, Ornella Bimai, Pierre Legrand, Sylvain Caillat, Jean-Luc Ravanat, et al.. Nonredox thiolation in tRNA occurring via sulfur activation by a [4Fe-4S] cluster. Proceedings of the National Academy of Sciences of the United States of America, 2017, 114 (28), pp.7355-7360. 10.1073/pnas.1700902114 . hal-02410958

HAL Id: hal-02410958
https://hal.science/hal-02410958

Submitted on 14 Dec 2019

HAL is a multi-disciplinary open access archive for the deposit and dissemination of scientific research documents, whether they are published or not. The documents may come from teaching and research institutions in France or abroad, or from public or private research centers.

L'archive ouverte pluridisciplinaire **HAL**, est destinée au dépôt et à la diffusion de documents scientifiques de niveau recherche, publiés ou non, émanant des établissements d'enseignement et de recherche français ou étrangers, des laboratoires publics ou privés.

Nonredox thiolation in tRNA occurring via sulfur activation by a [4Fe-4S] cluster

Simon Arragain[a,1], Ornella Bimai[a,1], Pierre Legrand[b], Sylvain Caillat[c], Jean-Luc Ravanat[c], Nadia Touati[d], Laurent Binet[d,e], Mohamed Atta[f], Marc Fontecave[a,2], and Béatrice Golinelli-Pimpaneau[a,2]

[a]Laboratoire de Chimie des Processus Biologiques, Unité Mixte de Recherche 8229 CNRS, Collège de France, Université Pierre et Marie Curie, 75231 Paris cedex 05, France; [b]SOLEIL Synchrotron, L'Orme des Merisiers, 91198 Gif-sur-Yvette, France; [c]University of Grenoble Alpes, Commissariat à l'Energie Atomique, Institut Nanosciences et Cryogénie, Systèmes Moléculaires et Nanomatériaux pour l'Energie et la Santé, F-38054 Grenoble, France; [d]CNRS Institut de Recherche Renard, Chimie-ParisTech, 75005 Paris, France; [e]Paris Sciences et Lettres Research University, Chimie-ParisTech, Institut de Recherche de Chimie-Paris, 75005 Paris, France; and [f]University of Grenoble Alpes, Commissariat à l'Energie Atomique, Direction de Recherche Fondamentale, Institut de Biosciences et Biotechnologies de Grenoble, Laboratoire Chimie et Biologie des Métaux, Unité Mixte de Recherche 5249, F-38000 Grenoble, France

Edited by Wolfgang Buckel, Max Planck Institut für terrestrische Mikrobiologie, Marburg, Germany, and accepted by Editorial Board Member Stephen J. Benkovic June 5, 2017 (received for review January 20, 2017)

Sulfur is present in several nucleosides within tRNAs. In particular, thiolation of the universally conserved methyl-uridine at position 54 stabilizes tRNAs from thermophilic bacteria and hyperthermophilic archaea and is required for growth at high temperature. The simple nonredox substitution of the C2-uridine carbonyl oxygen by sulfur is catalyzed by tRNA thiouridine synthetases called TtuA. Spectroscopic, enzymatic, and structural studies indicate that TtuA carries a catalytically essential [4Fe-4S] cluster and requires ATP for activity. A series of crystal structures shows that (*i*) the cluster is ligated by only three cysteines that are fully conserved, allowing the fourth unique iron to bind a small ligand, such as exogenous sulfide, and (*ii*) the ATP binding site, localized thanks to a protein-bound AMP molecule, a reaction product, is adjacent to the cluster. A mechanism for tRNA sulfuration is suggested, in which the unique iron of the catalytic cluster serves to bind exogenous sulfide, thus acting as a sulfur carrier.

tRNA modification | thiolation | [Fe-S] cluster | thiouridine synthetase | U54–tRNA

The cellular translation machinery contains essential components such as tRNAs. To achieve their function, they feature a great variety of well-conserved posttranscriptional chemical modifications. Sulfur is present in several of these modified nucleosides: thiouridine and derivatives (s^4U8, s^2U34, and m^5s^2U54), 2-thioadenosine derivatives (ms^2i^6A37 and ms^2t^6A37), and 2-thiocytidine (s^2C32). However, mechanisms of sulfur insertion into tRNAs are largely unknown, and the enzymes responsible for these reactions are incompletely characterized. Whereas redox conversion of a C-H to a C-S bond (synthesis of ms^2i^6A37 and ms^2t^6A37) depends on redox enzymes from the Radical-*S*-adenosyl-L-methionine iron-sulfur enzyme family, simple nonredox conversion of C = O to C = S group (synthesis of s^2U34 and s^4U8) is not expected to require such redox clusters. Intriguingly, we recently discovered that the ATP-dependent formation of s^2C32 in some tRNAs is catalyzed by an iron-sulfur enzyme, TtcA (1). However, the role of its cluster has not been defined. In the same superfamily, TtuA enzymes catalyze the C2-thiolation of uridine 54 in the T loop of thermophilic tRNAs (Fig. 1*A*), allowing stabilization of tRNAs at high temperature in thermophilic microorganisms. Sequences analysis shows that they share conserved cysteines and ATP binding motif (Fig. S1). Here, we report a detailed biochemical and structural characterization of TtuA that shows the presence of a [4Fe-4S] cluster essential for activity. The crystal structures of *Pyrococcus horikoshii* TtuA (PhTtuA) show that the cluster, chelated by only three cysteines, is adjacent to the ATP binding site. The presence of electron density near the fourth iron, nonbonded to the protein, indicates that the cluster can bind an exogenous substrate. We propose that thiolation occurs via sulfur binding to the cluster and transfer to the tRNA substrate. The fact that the catalytic [4Fe-4S] cluster serves as a sulfur carrier during a nonredox thiolation reaction illustrates an unknown function in iron-sulfur enzymology.

Results

m^5s^2U but Not s^2C Is Present in tRNAs from *Thermotoga maritima*. In the *Thermotoga maritima* genome, only one homolog of the *ttuA* gene was detected (2). It was earlier suggested that TtuA could perform thiolation of both C32 and m^5U54 in this organism (2), because both s^2C and m^5s^2U were detected in bulk tRNAs (3). However, our results show that, although 10.7 m^5s^2U modifications per 1,000 uridines were detected, both m^5U and s^2C were under the threshold of detection (below one modification per million normal nucleosides) (Fig. S2).

***T. maritima* TtuA Binds an [Fe-S] Cluster.** Recombinant *T. maritima* TtuA (TmTtuA) was purified as an apoprotein, apo-TmTtuA (Fig. 2*A* and Fig. S3*A*), then anaerobically treated with ferrous iron and L-cysteine in the presence of a cysteine desulfurase, and finally, purified (Fig. S3*B*) in the form of a homogeneous dimeric brownish protein, named holo-TmTtuA. Metal analysis (1.6 ± 0.1 Zn, 3.1 ± 0.2 Fe, and 2.6 ± 0.3 S per monomer) and UV-visible as well as EPR spectroscopy (Fig. 2) show that one TmTtuA monomer binds

Significance

Posttranscriptional modifications of tRNA are essential for translational fidelity. More specifically, mechanisms of selective sulfuration of tRNAs are still largely unknown, and the enzymes responsible for these reactions are incompletely investigated. Therefore, characterizing such systems at the molecular level is greatly valuable to our understanding of a whole class of tRNA modification reactions. We study TtuA, a representative member of a tRNA modification enzyme superfamily, and show that it intriguingly catalyzes a nonredox sulfur insertion within tRNA using a catalytically essential [4Fe-4S] cluster. This report opens perspectives regarding functions of iron-sulfur proteins in biology as well as chemical reactions catalyzed by iron-sulfur clusters.

Author contributions: M.F. and B.G.-P. designed research; S.A., O.B., P.L., S.C., J.-L.R., N.T., L.B., M.A., and B.G.-P. performed research; S.A., O.B., P.L., J.-L.R., L.B., M.F., and B.G.-P. analyzed data; and S.A., M.F., and B.G.-P. wrote the paper.

The authors declare no conflict of interest.

This article is a PNAS Direct Submission. W.B. is a guest editor invited by the Editorial Board.

Data deposition: The coordinates and structure factors have been deposited in the Protein Data Bank, www.pdb.org (PDB ID codes 5MKO, 5MKP, and 5MKQ for the AMP, FeS, and FeS-ano structures, respectively).

[1]S.A. and O.B. contributed equally to this work.

[2]To whom correspondence may be addressed. Email: marc.fontecave@cea.fr or beatrice.golinelli@college-de-france.fr.

This article contains supporting information online at www.pnas.org/lookup/suppl/doi:10.1073/pnas.1700902114/-/DCSupplemental.

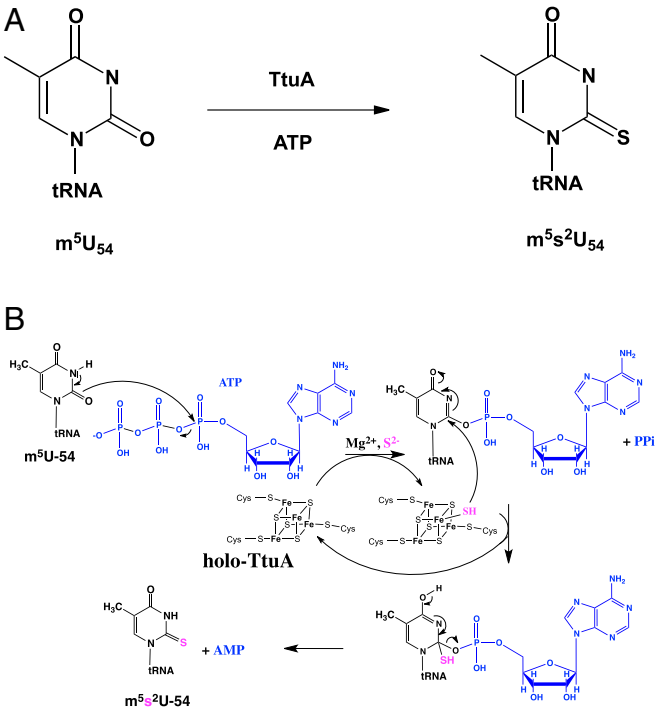

Fig. 1. (*A*) Thiolation reaction catalyzed by TtuA. (*B*) Proposed thiolation mechanism of TtuA with the [4Fe-4S] cluster playing the role of sulfur carrier, allowing multiple catalytic cycles. In the TtuA–tRNA complex, m^5U54 would bind in the site containing ATP and the cluster, coordinated by the sulfur (SH) cosubstrate. After adenylation at O^2, nucleophilic substitution of *O*-adenosyl monophosphate by SH would generate the final product m^5s^2U54.

two Zn atoms and one redox-active [4Fe-4S] cluster. Oxidized holo-TtuA is in an S = 0 EPR-silent $[4Fe\text{-}4S]^{2+}$ state, with an absorption band at 400 nm that disappears on reduction by dithionite (Fig. 2*A*), whereas reduced holo-TtuA is in an S = 1/2 $[4Fe\text{-}4S]^{+}$ state as shown by the rhombic EPR signal centered at $g = 1.93$ (0.63 ± 0.05 spin per monomer) (Fig. 2*B*).

The [4Fe-4S] Cluster Is Required for m^5U54 Thiolation. The thiolation activity of TmTtuA (1 μM) was assayed at 65 °C using 1 mM sodium sulfide as the sulfur source in the presence of ATP and Mg^{2+}. Bulk tRNA (10 μM) from the *ttcA*$^-$ *Escherichia coli* strain, lacking s^2C and m^5s^2U, was used as the substrate. Both substrate (m^5U) and product (m^5s^2U) were monitored by HPLC after tRNA digestion (Fig. 3). Holo-TtuA was unambiguously shown to be active for converting m^5U into m^5s^2U (0.22 nmol m^5s^2U min^{-1} per 1 nmol protein) (Fig. 3 *B* and *C* and Fig. S3 *C* and *D*). The reaction stopped after 30 min (after seven turnovers), likely as a consequence of enzyme inactivation. This inactivation was not caused by degradation of the cluster, because the UV-visible spectrum of the enzyme after reaction still displayed the band at 400 nm, characteristic of the [4Fe-4S] cubane (Fig. S3*E*). Furthermore, addition of thermostable pyrophosphatase did not increase the number of turnovers, indicating that pyrophosphate is not an enzyme inhibitor. No s^2C formation was detected, and no formation of m^5s^2U could be observed when (*i*) holo-TtuA was replaced by apo-TtuA (Fig. S3 *C* and *D*) or (*ii*) Mg^{2+}, ATP, or sulfide was excluded from the assay mixture (Fig. S3 *C* and *D*). The enzyme reduced with dithionite had an activity comparable with that of nonreduced holo-TmTtuA (Fig. S3*C*). Altogether, these experiments showed that, although the [4Fe-4S] cluster is essential for activity, it is not itself the source of sulfur atoms. To further confirm that the sulfur atom incorporated in the tRNA comes from the exogenous source, we carried out the TtuA activity assay in the presence of ^{35}S-sulfide generated by cysteine desulfurase in the presence of ^{35}S-L-cysteine. The results show that labeled sulfur is incorporated in the tRNA, showing that TtuA uses the added sulfur source as substrate (Fig. S3*F*).

Because we failed to crystallize TmTtuA, we also purified PhTtuA as reported elsewhere (4) (Fig. S4 *A* and *B*) and used the same [Fe-S] cluster reconstitution protocol as for TmTtuA. The presence of a [4Fe-4S] cluster was confirmed by UV-visible spectroscopy (Fig. S4*C*), and the enzyme, assayed at 85 °C (because of the high-growth temperature of *P. horikoshii*), proved to be enzymatically active but less than holo-TmTtuA (0.02 min^{-1}) (Fig. S4*D*).

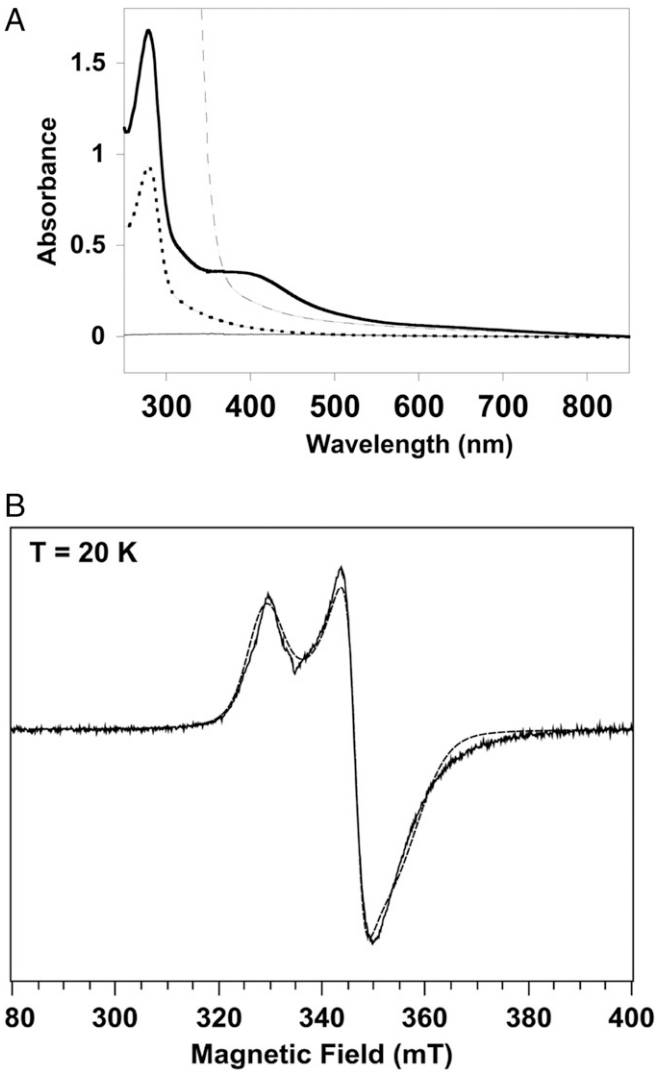

Fig. 2. Spectroscopic characterization of TmTtuA. (*A*) UV-visible spectra of apo-TmTtuA (dotted line), holo-TmTtuA (thick line), and reduced holo-TmTtuA after 1 min of incubation with 1 mM dithionite (dashed line). The spectra were recorded with 40 μM protein in Tris·HCl, pH 8, and 200 mM NaCl. (*B*) X-band EPR spectrum of reduced holo-TmTtuA at 20 K. The experimental (solid line) and simulated (dashed line) spectra are superimposed. A large background signal was removed from the experimental spectrum by polynomial interpolation. In the simulation, a g matrix with three distinct principal values, $g_x = 1.890$, $g_y = 1.935$, and $g_z = 2.040$, was used as well as a Lorentzian shape with 2 mT width for the individual transitions. In addition, anisotropic Gaussian broadenings with full-widths at half-height ΔBx = 11 mT, ΔBy = 2 mT, and ΔBz = 6 mT were introduced.

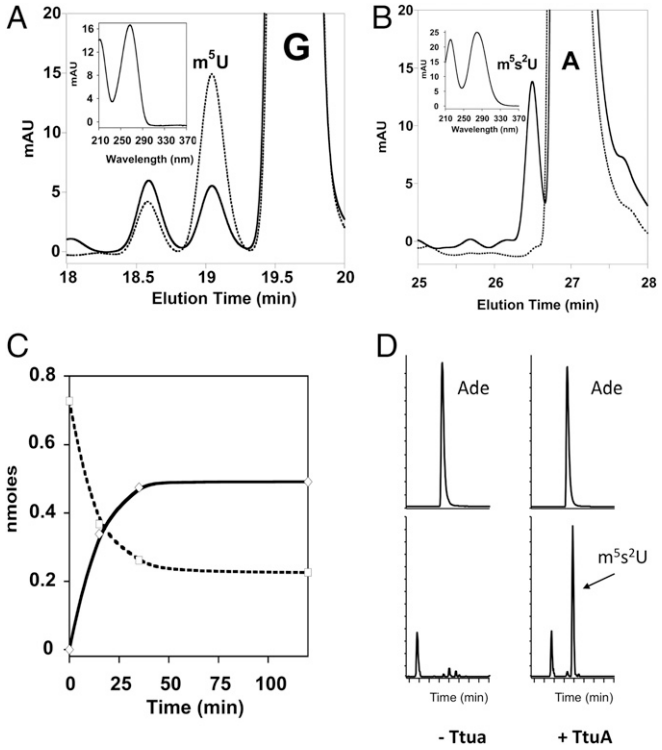

Fig. 3. In vitro thiolation activity of TmTtuA. The thiolation activity of TmTtuA was tested using *ttcA*$^{-}$ *E. coli* bulk tRNA as substrate. After digestion of the tRNA product, the modified nucleosides were analyzed by HPLC by following absorption at 260 nm. Elution profiles on an SB-C18 column between 18–20 (*A*) and 25–28 min (*B*) at $t = 0$ (dotted line) and $t = 120$ min (solid line) of reaction. m^5U eluates at 19.5 min (*A*) and m^5s^2U at 26.6 min (*B*). The UV-visible spectrum characteristic of each modified nucleoside is shown in *Insets*. (*C*) Time course of m^5U consumption (dashed line) and m^5s^2U synthesis (solid line). (*D*) HPLC-MS/MS detection of m^5s^2U in tRNA. (*Upper*) Analysis of adenosine (Ade) as an internal control. (*Lower*) Analysis of m^5s^2U using the transition *m/z* 275→143. (*Left*) Untreated tRNA. (*Right*) tRNA treated with TmTtuA in the presence of sulfide.

In *P. horikoshii* Holo-TtuA, a [4Fe-4S] Cluster Is Chelated by Three Conserved Cysteines, with the Fourth Unique Iron Being Able to Bind Sulfide. Here, we report three different crystal structures of PhTtuA: one in space group $P4_32_12$ with one molecule in the asymmetric unit and two in space group $P2_12_12_1$ with two molecules in the asymmetric unit (Fig. 4 and Table S1). Their overall structure is identical to that of the apoprotein (4). Monomers are superimposable, and all contain two Zn atoms at the N and C termini bound by conserved cysteines and one histidine (Fig. 4). The dimer is formed between either two molecules in the asymmetric unit or two symmetric molecules, with the interface provided by hydrophobic residues (Fig. S5).

The "FeS" holoenzyme structure, solved at 2.5-Å resolution, contains the [4Fe-4S] cluster, which is chelated by only three conserved cysteines, Cys128, Cys131, and Cys220, and surrounded by hydrophobic residues (Leu81, Ile83, and Ile118) (Fig. 5*A* and Fig. S6*A*). In the apoprotein, Cys128 and Cys220 were linked by a disulfide bond (Fig. 5*A*) (4). The nature of the cluster was confirmed by the "FeS-ano" structure collected at the iron K edge, for which the anomalous difference map displays clear electron density corresponding to a [4Fe-4S] cluster close to the three central conserved cysteines (Fig. S7*A*). In the FeS structure, an extra electron density is present near the fourth iron atom of the cluster (nonprotein bonded) (Fig. 5*B* and Fig. S8). This density can be equally well-fitted by a hydroxide or a hydrosulfide ion. However, this site, in a mostly hydrophobic environment at a distance of 2.4 Å from the unique iron atom and 3.2 Å from the positively charged amino group of Lys135, is appropriate to accommodate a hydrosulfide ligand. Interestingly, the conformation of Lys135 is different in holo- and apo-PhTtuA (Fig. 5*A*). A lysine or arginine is always present at this position in the TtuA superfamily (Fig. S1), suggesting an important function for this residue.

AMP Is Bound to PhTtuA at the ATP Binding Site, Which Is Located Close to the [Fe-S] Cluster Site. The third "AMP" structure contains an AMP molecule, which seems to have copurified with the protein (Fig. 5*C* and Fig. S6*B*). The [4Fe-4S] cluster in the two molecules of the asymmetric unit seems to be degraded to [2Fe-2S] clusters (Fig. S7*B*). Superposition of the three structures shows that AMP and the cluster are 4.3 Å away from each other with Lys135 in between (Figs. 4 and 5*D*). In all structures, residues 222–225 near catalytic Cys220 are disordered, like in apo-PhTtuA (4) (Fig. 4). These residues would likely get ordered in the presence of the tRNA substrate. The residues involved in AMP binding belong to the PP-loop motif characteristic of ATPases (Fig. 5*C* and Fig. S1) (5), indicating that the essential ATP cofactor binds at the same site.

TtuA Displays a High Structural Similarity with Lysidine Synthetase. Interestingly, TtuA shows the highest structural similarity with lysidine synthetase (TilS) (6), an *N*-type ATP pyrophosphatase (Z score = 10.7 as determined by the European Molecular Biology Laboratory, European Bioinformatics Institute, Secondary Structure Matching server). The structure of TilS has been determined in complex with either ATP (7) or the tRNA substrate (6). The superposition of the ATP binding sites of TilS and TtuA indicates how ATP and Mg^{2+} are likely accommodated in the TtuA active site (Fig. S9 *A* and *B*). Arg113 and His133 in TilS interact with the β- and γ-phosphate groups of ATP (7). The corresponding residues in TtuA, Lys135 and His155, likely have the same function. Superposition with the structure of tRNA–TilS complex shows that the anticodon stem loop occupies the cavity created by the assembly of two TtuA monomers without

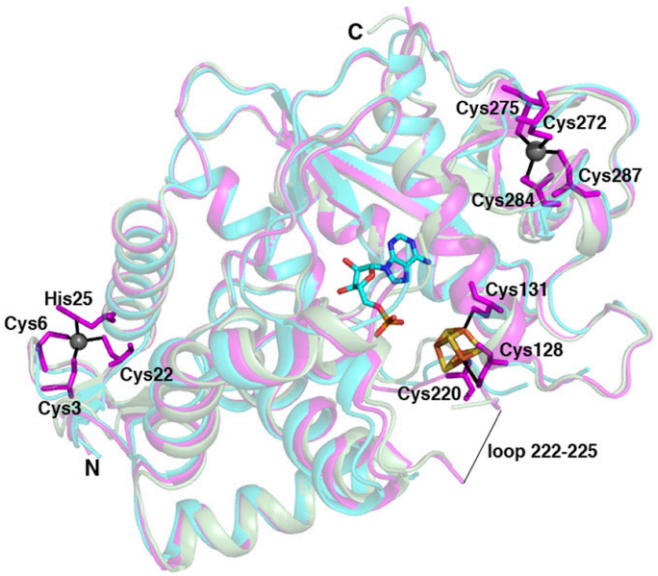

Fig. 4. Superposition of the three PhTtuA structures. One monomer of the AMP or FeS-ano structures (colored cyan and magenta, respectively) was superimposed with the FeS structure in pale green (rmsd of 0.30 Å for 238 atoms and 0.50 Å for 257 Cαs, respectively). AMP is shown in cyan. The zinc atoms are shown as gray spheres, and cysteines involved in [Fe-S] or Zn binding as well as the [4Fe-4S] of the FeS structure are shown as sticks. The N and C termini are indicated as N and C, respectively, and the position of unstructured loop 222–225 is shown as a thin black line.

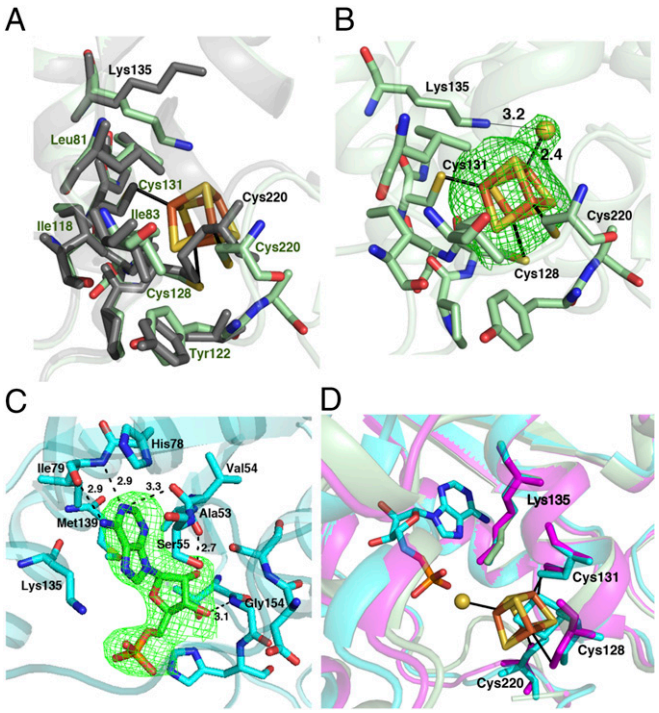

Fig. 5. The [Fe-S] cluster and AMP ligands occupy close positions within the TtuA active site. (*A*) Superposition of the FeS structure (pale green) on apo-PhTtuA (PDB ID code 3VRH; gray). In apo-PhTtuA, Cys220 and Cys128 form an intramolecular disulfide bond. (*B*) Fo-Fc difference map omitting the [4Fe-5S] cluster contoured at 2σ (green) superimposed on the [Fe-S] site of the FeS structure. The occupancies of the coordinating sulfur atom and the unique iron have been estimated to be 0.7. (*C*) Active site of the AMP structure. An Fo-Fc electron density map omitting the AMP ligand (green) contoured at 3σ is superimposed on the active site. The adenine ring is stacked between the side chains of Lys135 and Ser55, and the H bonds between the hydroxyl group of Ser55 and the NH groups of Gly56 and Gly57 within the PP-loop motif create a sharp turn that likely plays a structural role (32). (*D*) Superposition of the active site of three structures. The [2Fe-2S] cluster of the AMP structure is shown in cyan.

creating any clashes and that the flipped C34 target base of TilS is adjusted finely to the TtuA active site pocket (Fig. S9 *C* and *D*). This superposition suggests the formation of a flipped adenylated uridine intermediate at the target position during TtuA catalysis. Because TilS does not target the T-stem loop but C34 in the anticodon loop, the tRNA is obviously not expected to bind to TtuA, as shown in Fig. S9*C*, but we anticipate the T-stem loop to be bound to TtuA in a similar manner. Superposition of TtuA and TilS also suggests that two tRNA molecules are likely bound on each side of one TtuA dimer and that the two zinc finger domains belonging to different polypeptide chains of TtuA may be used to clamp the T-stem loop on opposite sides. Such a positioning of tRNA relative to the TtuA dimer is in agreement with the complementary electrostatic surface between the highly positively charged putative tRNA binding site (Fig. S9*E*) and the negatively charged tRNA substrate.

Discussion

Several intriguing questions can be addressed on the basis of the crystal structures reported here. The first one regards the source of sulfur atoms. A well-established thiolation mechanism, occurring in the case of s^2U34 (MnmA) and s^4U8 (ThiI) formation in tRNAs, involves a persulfide carried by an active site cysteine as the sulfurating agent (8–10). The 3D structure of TtuA allows us to exclude such a mechanism, because no free cysteine, as a potential site for a catalytic persulfide, can be observed in the active site (Fig. 4). Indeed, the conserved cysteines in TtuA enzymes are bound to either the [Fe-S] cluster or the Zn ions (Fig. 4 and Fig. S1). In a second mechanism, the sulfur comes from the C-terminal thiocarboxylated enzyme as in the case of molybdopterin (11) and thiazole (12) biosynthesis. It is excluded that the sulfur that is inserted into the nucleoside comes from the C-terminal carboxylate of TtuA, because it is far away from the active site (Fig. 4). We here show that free sulfide sustains thiolation of uridine under in vitro conditions. It is tempting to suggest that it is also the sulfur source in vivo. Free sulfide has been shown to be present at relatively high concentrations within thermophilic archaea (13) and participate in [Fe-S] cluster assembly as well as biosynthesis of methionine (14), thiamin thiazole (15), and U8–tRNA thiolation (16).

The second question is the role of the [Fe-S] cluster in TtuA and also, TtcA, which catalyzes formation of s^2C32 in some tRNAs (1). In Fig. 1*B*, we propose a reaction mechanism based on the following facts. First, because TtuA is not functional in the absence of sulfide, sulfur atoms from the cluster itself cannot be used as the substrate. Second, labeling experiments indicated that ^{35}S-sulfur is incorporated into tRNA when the TtuA reaction is run in the presence of ^{35}S-sulfide generated by cysteine desulfurase. Third, the cluster of TtuA is ligated by only three cysteines and thus, has a free coordination site on the fourth iron, which can be occupied by a hydrosulfide ligand. Precedents for exogenous sulfur species bound to an iron site of a [4Fe-4S] cluster have been reported: a comparable [4Fe-5S] cluster has been observed in HydG, an enzyme involved in maturation of hydrogenases (17), as well as 2-hydroxyisocaproyl-CoA dehydratase (18). Moreover, in the structure of the methylthiotransferase RimO, a polysulfide terminal ligand to a [4Fe-4S] cluster has been observed (19).

Fourth, the cluster is adjacent to the ATP binding site, and the structural similarity with TilS indicates that the target uridine can be positioned in close proximity to the ATP-cluster active site.

We propose that the active site serves to bring the adenylated m^5U–tRNA substrate close to a reactive hydrosulfide attached to the cluster. Adenylation of uridine seems to be a general mechanism for activation (9, 20), and would facilitate a nucleophilic attack of the hydrosulfide to C2 of m^5U (Fig. 1*B*). Furthermore, such similar addition of an Fe-SH nucleophile to a carbonyl group has been shown to occur during thiazole formation catalyzed by Fe-dependent archaeal thiazole synthases (21). Elimination of AMP then generates the final m^5s^2U–tRNA product. We open the possibility that this mechanism applies to other members of the TtcA/TtuA thiolase enzyme superfamily, sharing the three conserved cysteine ligands (Fig. S1), such as Ncs6/Ctu1 enzymes targeting uridine-34 and some archaeal ThiI enzymes targeting uridine-8 in tRNAs (22).

Material and Methods

Cloning of the *ttua* Genes. The *T. maritima* gene coding for the TM0197 protein was amplified by PCR from genomic *T. maritima* MS8 DNA by the pfu DNA polymerase using the following primers: 5′-AAAGGAGGGAAA**CATATG**AAGTGTACCAAG-3′ (NdeI site bolded and ATG codon underlined) and 5′-AAAATGATCCC**AAGCTT**ATGCGGGGGTTTT-3′ (HindIII site bolded) hybridized to the coding strand at the TGA stop codon. The amplified product was cloned into the pT7-7 plasmid, giving the *pT7-7-ttuA* plasmid. The gene encoding the PH0300 TtuA protein from *P. horikoshii* was synthesized by GenScript with codon optimization for *E. coli* and subcloned into the pBG102 plasmid (pET27 derivative) between the BamHI and EcoRI restriction sites to produce a 6His-SUMO-TtuA protein construct.

Overexpression of TmTtuA. The plasmid containing the *ttuA* gene was transformed into *E. coli* BL21(*DE3*) star codon$^+$-competent cells. One colony was used to inoculate 100 mL of Luria Broth medium supplemented with ampicillin (100 μg/mL) and chloramphenicol (30 μg/mL); 50 mL of this preculture grown overnight at 37°C was used to inoculate 10 L of Luria Broth medium supplemented with the same antibiotics. Cultures were grown at 37 °C to an OD_{600} of 0.6, and expression was induced at 30 °C by addition of isopropyl-β-D-thiogalactopyranoside (IPTG) to a final concentration of 1 mM. After 10 h, cells were collected by centrifugation; resuspended in 20 mM Tris·HCl, pH 8, and 200 mM NaCl; and stored at −80 °C.

Purification of TmTtuA. Cells were resuspended in 20 mM Tris·HCl, pH 8, 200 mM NaCl, and 0.1 mM phenylmethylsulfonyl fluoride and disrupted by sonication. Cells debris was removed by ultracentrifugation at 200,000 × *g* for 20 min at 4 °C, and the supernatant was heated at 75 °C for 15 min to precipitate the *E. coli* proteins. After centrifugation at 30,000 × *g* for 30 min at 4 °C and addition of ammonium sulfate (1.5 M final concentration), the supernatant was loaded on a 20-mL prepacked hydrophobic interaction chromatography resin (Butyl Sepharose fast flow; GE Healthcare). The column was washed with four column volumes of 20 mM Tris·HCl, pH 8, 200 mM NaCl, and 1.5 M ammonium sulfate and eluted with a linear gradient of 1.5–0 M ammonium sulfate. Fractions containing the TmTtuA protein were then loaded on a Superdex 200 10/300 column (GE Healthcare) equilibrated in 20 mM Tris·HCl, pH 8, 200 mM NaCl, and 5 mM DTT. The protein was concentrated to 30 mg/mL using Amicon concentrators (30-kDa cutoff; Milllipore), aliquoted, frozen in liquid nitrogen, and stored at −80 °C.

Overexpression and Purification of PhTtuA. The plasmid containing the *ttuA* gene was overexpressed in *E. coli* BL21 (DE3). Cells (6 L) were grown at 37 °C in Luria Broth medium supplemented with kanamycin (50 μg/mL) to an OD_{600} of 1.2. Protein expression was then induced with 1 mM IPTG, and incubation was extended overnight at 20 °C. After centrifugation, pellets were resuspended in 10 mL of 50 mM NaH_2PO_4, pH 7.5, 500 mM NaCl, 40 mM imidazole with RNase A (2 μg/mL), and benzonase and disrupted by sonication. Cells debris was removed by ultracentrifugation at 210,000 × *g* for 1 h at 4 °C. The supernatant was then loaded on an immobilized metal affinity Ni-NTA column (HisTrap 5 mL; GE Healthcare) equilibrated in 50 mM NaH_2PO_4, pH 7.5, 500 mM NaCl, and 40 mM imidazole and eluted with a linear gradient of 0–1 M imidazole. The protein was collected; dialyzed overnight against 50 mM Tris·HCl, pH 7.5, and 150 mM NaCl in the presence of the PreScission Protease (150 μM); centrifugated at 4 °C for 10 min; and then, loaded on a MonoS cation exchange column (GE Healthcare) using an AKTA system at 1 mL min^{-1}. Elution was performed with a linear gradient of 0.02–1 M NaCl in the same buffer for 20 min. Fractions containing the TtuA protein were concentrated and loaded on a gel filtration column (Hiload 16/60 Superdex S200; GE Healthcare) in 25 mM Hepes, pH 7.5, 200 mM NaCl, and 5 mM DTT. The purified protein was concentrated to 15 mg/mL with an Amicon Ultra filter device (30-kDa cutoff; Millipore), frozen in liquid nitrogen, and stored at −80 °C. The GST–3C-protease (PreScission) was expressed using pGEX-2T recombinant plasmids. After induction at 25 °C with 0.1 mM IPTG for 20 h, the protein was purified using glutathione–Sepharose chromatography.

[Fe-S] Cluster Reconstitution and Purification of Holo-TtuA Proteins. The reconstitution of the [4Fe-4S] cluster and purification of holo-TmTtuA and holo-PhTtuA were performed under strict anaerobic conditions in an Mbraun glove box containing less than 0.5 ppm O_2. TtuA was treated with 5 mM DTT for 10 min and then incubated overnight with a fivefold molar excess of ferrous ammonium sulfate and L-cysteine in the presence of 2 μM *E. coli* cysteine desulfurase CsdA. The holo-TtuA was then loaded onto a Superdex 200 10/300 gel filtration column (GL Sciences) equilibrated in 20 mM Tris·Cl, 200 NaCl, and 5 mM DTT. The peak containing the TtuA dimer was then concentrated to 15–25 mg/mL on a Vivaspin concentrator (30-kDa cutoff).

Quantification Methods. The Pierce BCA assay was used to quantify the protein (23). Inductively coupled plasma atomic emission spectroscopy (Shimadzu ICP 9000 instrument with mini plasma torch in axial reading mode) was used to detect and quantify zinc and iron in TmTtuA. Standard solutions of zinc and ytterbium for atomic absorption spectroscopy (Sigma-Aldrich) were used for quantification [calibration curve between 10 and 500 μg/L with 1% HNO_3 (Fluka)]. Ytterbium was used as an internal standard to prevent calibration drift and fluidic perturbation. The Fish (24) and Beinert (25) methods were routinely used to quantify iron and sulfide, respectively, after cluster reconstitution.

Preparation of Bulk tRNA. Bulk tRNA was purified from either MS8 *T. maritima* or GRB 105 *ttcA*$^-$ *E. coli* cells as described (26).

In Vitro Enzymes Assay. The reaction mixture contained in 100 μL 25 mM Tris·HCl, pH 8, 200 mM NaCl, 1 mM ATP, 5 mM $MgCl_2$, 10 μM *E. coli ttcA*$^-$ bulk tRNA, 1 mM Na_2S, and 1 μM TtuA. After 1 h of incubation at 65 °C (TmTtuA) or 85 °C (PhTtuA) under anaerobic conditions, the tRNA products were digested and analyzed by HPLC. Thermostable inorganic pyrophosphatase from *Thermococcus litoralis* was bought from New England Biolabs (M0296L). For the labeling experiment, ^{35}S-sulfide was first formed by incubating 500 μM L-cysteine in the presence of 10, 25, or 50 μCi of ^{35}S-L-cysteine in 50 μL of solution containing 25 mM Tris·HCl, pH 8, 200 mM NaCl, 5 mM 1,4-DTT, and 4 μM *E. coli* cysteine desulfurase CsdA. After 2 h of reaction at 37 °C under nitrogen atmosphere, the thiolation activity of TmTtuA (1 μM) was assayed by incubating the ^{35}S-sulfide–containing mixture with 50 μL of solution containing *ttcA*$^-$ *E. coli* bulk tRNA (10 μM), ATP (500 μM), and Mg^{2+} (5 mM) for 1 h at 65 °C under nitrogen atmosphere. Finally, RNA was separated by PAGE on a 12% (wt/vol) gel containing 7 M urea. The gel was stained with 0.025% (wt/vol) toluidine blue, then dried, and visualized by phosphor imaging with a Typhoon apparatus (GE Healthcare).

tRNA digestion and quantification of modified nucleosides. For tRNA digestion, 10 μM tRNA was digested overnight in 100 μL of 25 mM Tris·HCl, pH 8, 200 mM NaCl, and 0.1 mM $ZnSO_4$ at 37 °C by nuclease P1 (2 U; Sigma-Aldrich) followed by the addition of alkaline phosphatase during 2 h at 37 °C (2 U; Sigma-Aldrich). After an initial unambiguous identification of the elution position of the modified nucleosides by HPLC-MS/MS, quantification of the modified nucleosides was routinely performed as follows. The nucleosides products were injected on an SB-C18 HPLC column (Agilent Technologies) mounted with an SB-C18 precolumn connected to a binary HPLC system (1260 Infinity; Agilent Technologies). The Gehrke and Kuo (27) gradient was used to separate the different nucleosides and quantify m^5U and m^5s^2U.

HPLC-MS/MS analysis of modified nucleosides. HPLC–tandem MS analyses were performed with an Accela chromatographic system coupled with a Quantum ultratriple quadripolar apparatus (Thermo Electron SAS) equipped with an HESI electrospray source used in the positive ionization mode. HPLC separation was carried out with a 2 × 150-mm octadecylsilyl silica gel (3-mm particle size) column (Uptisphere) and a 0–15% linear gradient of acetonitrile in 2 mM ammonium formate over 20 min as the mobile phase. MS detection was carried out in multiple reactions monitoring mode to obtain high sensitivity and specificity with settings optimized to favor loss of ribose on collision-induced fragmentation. The transitions used to detect the nucleosides were *m/z* 244→112 for cytidine, 260→128 for s^2C, 259→127 for s^2U, and 275→143 for m^5s^2U. Elution occurs at 6.0, 8.0, 10.2, and 14.8 min for cytidine, s^2C, s^2U, and m^5s^2U, respectively. Quantification was performed by external calibration.

[Fe-S] Cluster Characterization by UV-Visible Spectroscopy and EPR. UV-visible absorption spectra were recorded in quartz cuvettes (1-cm optic path) under anaerobic conditions in a glove box on a XL-100 Uvikon spectrophotometer equipped with optical fibers. TmTtuA was treated with 1 mM dithionite before recording the EPR spectrum. EPR spectra of TmTtuA were recorded in 707-SQ-250M tubes in 25 mM Tris·HCl, pH 8, and 200 mM NaCl on a Bruker ELEXSYS-E500 continuous-wave EPR spectrometer operating at 20 K with an SHQE cavity and an Oxford Instruments ESR900 helium flow cryostat under nonsaturating conditions using a microwave power of 4 mW, a microwave frequency of 9.3934 GHz, a modulation amplitude of 0.6 mT, a modulation frequency of 100 kHz, and an accumulation of 10 scans. For the determination of the number of unpaired spins, a Cu-EDTA (400 μM) standard sample was used. The simulation of the EPR spectrum was performed with the Easyspin software (www.easyspin.org/).

Crystallization, Data Collection, and Structure Determination. Crystals of holo-PhTtuA were obtained under anaerobic conditions with the same crystallization conditions as for the apoprotein (4). The AMP dataset corresponds to one minor lattice of some twinned crystals grown under the same anaerobic conditions. This lattice contained AMP, which had not been added in the crystallization solution, and a degraded form of the cluster. X-ray data were collected on a single crystal at 100 K at the SOLEIL synchrotron (Saint Aubin, France) on the Proxima1 and Proxima2 beamlines. Data were indexed, processed, and scaled with XDS (28). For the FeS and FeS-ano structures, noticeable anisotropy in the diffraction was taken into account and corrected by the programs DEBYE and STARANISO as accessible by the server staraniso.globalphasing.org/cgi-bin/staraniso.cgi. The apo-PhTtuA model [Protein Data Bank (PDB) ID code 3VRH] was used to solve the structures by molecular replacement with PHASER (29). BUSTER (30) was used for refinement, and COOT (31) was used for model reconstruction. Omit maps were calculated by omitting the ligand and using the MapOnly option in BUSTER. The presence of an extra electron density near the [4Fe-4S] cluster in the FeS structure was examined with datasets containing different numbers of images to take into account possible radiation damage. Weak extra electron density blobs present in the active site cavity could not be modeled with molecules present in the crystallization solution. Data collection and refinement statistics are given in Table S1. In all models, no residue has backbone dihedral angles in the forbidden region of the Ramachandran plot, and 97.02, 96.98, and 98.65% of the residues are in the favored region for the AMP, FeS-ano, and FeS structures, respectively.

ACKNOWLEDGMENTS. We thank Glen Björk for providing the *ttcA*$^-$ *E. coli* GRB105 strain; Stéphane Mouilleron for providing the plasmid encoding the GST–3C-protease; Dr. J. Pérard for quantification of zinc by inductively coupled plasma atomic emission spectroscopy; Martin Savko for assistance in using

beamline Proxima 2; Ludovic Pecqueur for maintenance of the glove boxes and advice in data treatment; Thibaut Fogeron and Xavier Itturioz for help in the labeling experiment with ^{35}S-L-Cysteine; Céline Brochier for performing genomic analysis; the Vanderbilt Center for Structural Biology for providing the pBG102 plasmid; the College de France for the Maître de Conférences Associé position (S.A.); the French EPR CNRS Facility, Infrastructure de Recherche Renard, Formation de Recherche en Evolution 3443 for the EPR experiments; and the SOLEIL synchrotron for provision of synchrotron radiation facilities. This work was supported by French State Program "Investissements d'Avenir" Grants "LABEX DYNAMO" and ANR-11-LABX-0011.

1. Bouvier D, et al. (2014) TtcA a new tRNA-thioltransferase with an Fe-S cluster. *Nucleic Acids Res* 42:7960–7970.
2. Shigi N, Sakaguchi Y, Suzuki T, Watanabe K (2006) Identification of two tRNA thiolation genes required for cell growth at extremely high temperatures. *J Biol Chem* 281:14296–14306.
3. Edmonds CG, et al. (1991) Posttranscriptional modification of tRNA in thermophilic archaea (Archaebacteria). *J Bacteriol* 173:3138–3148.
4. Nakagawa H, et al. (2013) Crystallographic and mutational studies on the tRNA thiouridine synthetase TtuA. *Proteins* 81:1232–1244.
5. Schmelz S, Naismith JH (2009) Adenylate-forming enzymes. *Curr Opin Struct Biol* 19: 666–671.
6. Nakanishi K, et al. (2009) Structural basis for translational fidelity ensured by transfer RNA lysidine synthetase. *Nature* 461:1144–1148.
7. Kuratani M, et al. (2007) Structural basis of the initial binding of tRNA(Ile) lysidine synthetase TilS with ATP and L-lysine. *Structure* 15:1642–1653.
8. Mueller EG, Palenchar PM, Buck CJ (2001) The role of the cysteine residues of ThiI in the generation of 4-thiouridine in tRNA. *J Biol Chem* 276:33588–33595.
9. Numata T, Ikeuchi Y, Fukai S, Suzuki T, Nureki O (2006) Snapshots of tRNA sulphuration via an adenylated intermediate. *Nature* 442:419–424.
10. Mueller EG (2006) Trafficking in persulfides: Delivering sulfur in biosynthetic pathways. *Nat Chem Biol* 2:185–194.
11. Wuebbens MM, Rajagopalan KV (2003) Mechanistic and mutational studies of *Escherichia coli* molybdopterin synthase clarify the final step of molybdopterin biosynthesis. *J Biol Chem* 278:14523–14532.
12. Jurgenson CT, Begley TP, Ealick SE (2009) The structural and biochemical foundations of thiamin biosynthesis. *Annu Rev Biochem* 78:569–603.
13. Jack Jones W, Paynter MJB, Gupta R (1983) Characterization of *Methanococcus maripaludis* sp. nov., a new methanogen isolated from salt marsh sediment. *Arch Microbiol* 135:91–97.
14. Liu Y, Sieprawska-Lupa M, Whitman WB, White RH (2010) Cysteine is not the sulfur source for iron-sulfur cluster and methionine biosynthesis in the methanogenic archaeon Methanococcus maripaludis. *J Biol Chem* 285:31923–31929.
15. Eser BE, Zhang X, Chanani PK, Begley TP, Ealick SE (2016) From suicide enzyme to catalyst: The iron-dependent sulfide transfer in Methanococcus jannaschii thiamin thiazole biosynthesis. *J Am Chem Soc* 138:3639–3642.
16. Liu Y, et al. (2012) Biosynthesis of 4-thiouridine in tRNA in the methanogenic archaeon *Methanococcus maripaludis*. *J Biol Chem* 287:36683–36692.
17. Dinis P, et al. (2015) X-ray crystallographic and EPR spectroscopic analysis of HydG, a maturase in [FeFe]-hydrogenase H-cluster assembly. *Proc Natl Acad Sci USA* 112: 1362–1367.
18. Knauer SH, Buckel W, Dobbek H (2011) Structural basis for reductive radical formation and electron recycling in (R)-2-hydroxyisocaproyl-CoA dehydratase. *J Am Chem Soc* 133:4342–4347.
19. Forouhar F, et al. (2013) Two Fe-S clusters catalyze sulfur insertion by radical-SAM methylthiotransferases. *Nat Chem Biol* 9:333–338.
20. You D, Xu T, Yao F, Zhou X, Deng Z (2008) Direct evidence that ThiI is an ATP pyrophosphatase for the adenylation of uridine in 4-thiouridine biosynthesis. *ChemBioChem* 9:1879–1882.
21. Cicchillo RM, Booker SJ (2005) Mechanistic investigations of lipoic acid biosynthesis in *Escherichia coli*: Both sulfur atoms in lipoic acid are contributed by the same lipoyl synthase polypeptide. *J Am Chem Soc* 127:2860–2861.
22. Liu Y, et al. (2016) A [3Fe-4S] cluster is required for tRNA thiolation in archaea and eukaryotes. *Proc Natl Acad Sci USA* 113:12703–12708.
23. Smith PK, et al. (1985) Measurement of protein using bicinchoninic acid. *Anal Biochem* 150:76–85.
24. Fish WW (1988) Rapid colorimetric micromethod for the quantitation of complexed iron in biological samples. *Methods Enzymol* 158:357–364.
25. Beinert H (1983) Semi-micro methods for analysis of labile sulfide and of labile sulfide plus sulfane sulfur in unusually stable iron-sulfur proteins. *Anal Biochem* 131:373–378.
26. Buck M, Ames BN (1984) A modified nucleotide in tRNA as a possible regulator of aerobiosis: Synthesis of cis-2-methyl-thioribosylzeatin in the tRNA of *Salmonella*. *Cell* 36:523–531.
27. Gehrke CW, Kuo KC (1989) Ribonucleoside analysis by reversed-phase high-performance liquid chromatography. *J Chromatogr* 471:3–36.
28. Kabsch W (2010) Xds. *Acta Crystallogr D Biol Crystallogr* 66:125–132.
29. Mccoy AJ, et al. (2007) Phaser crystallographic software. *J Appl Crystallogr* 40:658–674.
30. Bricogne G, et al. (2016) BUSTER (Global Phasing Ltd., Cambridge, UK), Version 2.10.2.
31. Emsley P, Lohkamp B, Scott WG, Cowtan K (2010) Features and development of Coot. *Acta Crystallogr D Biol Crystallogr* 66:486–501.
32. Nakanishi K, et al. (2005) Structural basis for lysidine formation by ATP pyrophosphatase accompanied by a lysine-specific loop and a tRNA-recognition domain. *Proc Natl Acad Sci USA* 102:7487–7492.
33. Chavarria NE, et al. (2014) Archaeal Tuc1/Ncs6 homolog required for wobble uridine tRNA thiolation is associated with ubiquitin-proteasome, translation, and RNA processing system homologs. *PLoS One* 9:e99104.
34. Liu Y, Long F, Wang L, Söll D, Whitman WB (2014) The putative tRNA 2-thiouridine synthetase Ncs6 is an essential sulfur carrier in *Methanococcus maripaludis*. *FEBS Lett* 588:873–877.
35. Noma A, Sakaguchi Y, Suzuki T (2009) Mechanistic characterization of the sulfur-relay system for eukaryotic 2-thiouridine biogenesis at tRNA wobble positions. *Nucleic Acids Res* 37:1335–1352.
36. Chowdhury MM, Dosche C, Lohmannsroben HG, Leimkuhler S (2012) Dual role of the molybdenum cofactor biosynthesis protein MOCS3 in tRNA thiolation and molybdenum cofactor biosynthesis in humans. *J Biol Chem* 287:17297–17307.
37. Sievers F, et al. (2011) Fast, scalable generation of high-quality protein multiple sequence alignments using Clustal Omega. *Mol Syst Biol* 7:539.
38. Gouet P, Courcelle E, Stuart DI, Metoz F (1999) ESPript: analysis of multiple sequence alignments in PostScript. *Bioinformatics* 15(4):305–308.
39. Krissinel E (2010) Crystal contacts as nature's docking solutions. *J Comput Chem* 31: 133–143.

Supporting Information

Arragain et al. 10.1073/pnas.1700902114

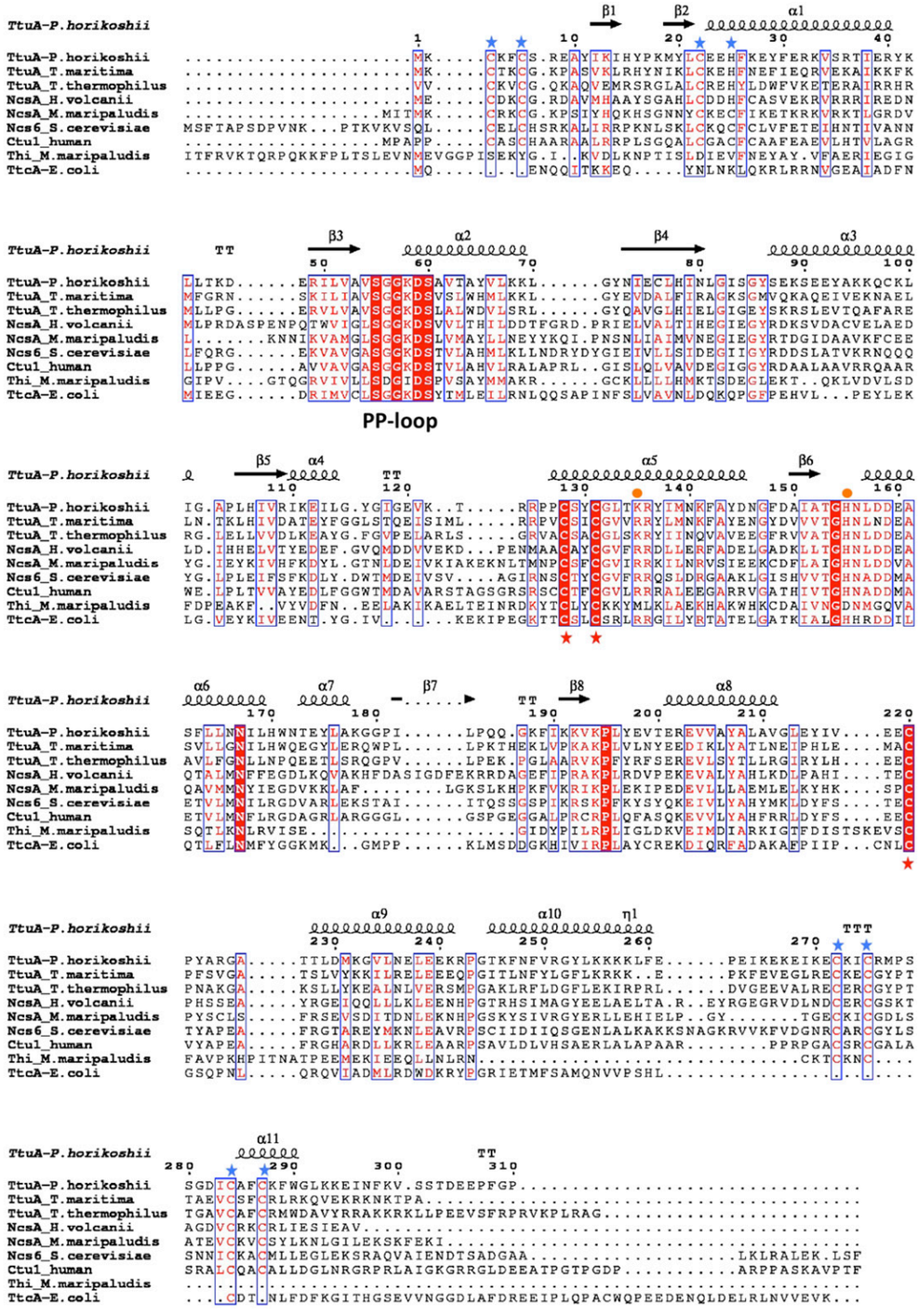

Fig. S1. Amino acid sequence alignment of several members of the TtcA/TtuA proteins superfamily. Alignment of protein sequences of the TtcA/TtuA superfamily: TtuA [from *Pyrococcus horikoshii* (PH0300) (4), *Thermotoga maritima* (TM0197), and *Thermus thermophilus* (TT_CO106) (4)], Ncs6 [from *Haloferax volcanii* (HVO_0580) (33), *Methanococcus maripaludis* (Mmp1356) (34), *Saccharomyces cerevisiae* (35), and human (36)], and *Escherichia coli* TtcA (1) were performed with Clustal Omega (37) and rendered with ESPript (38). ThiI from *M. maripaludis* is also indicated as an example of archaeal s^4U8 tRNA thiolase (22), but its 108 N-terminal residues have been omitted. The secondary structure elements of PhTtuA are shown above the alignment. All enzymes contain three conserved cysteines (indicated by red stars) that ligate the [4Fe-4S] cluster in TtcA and TtuA. The TtuA and Ncs6 subfamilies also contain two zinc finger motifs at the N and C termini that are highlighted by blue stars. The likely catalytic residues Lys135 and His155 are indicated as orange circles. It should be noted that the cysteines that coordinate the [Fe-S] cluster in TtuA are Cys122, Cys125, and Cys213, which are different from the previous incorrect numbering (1).

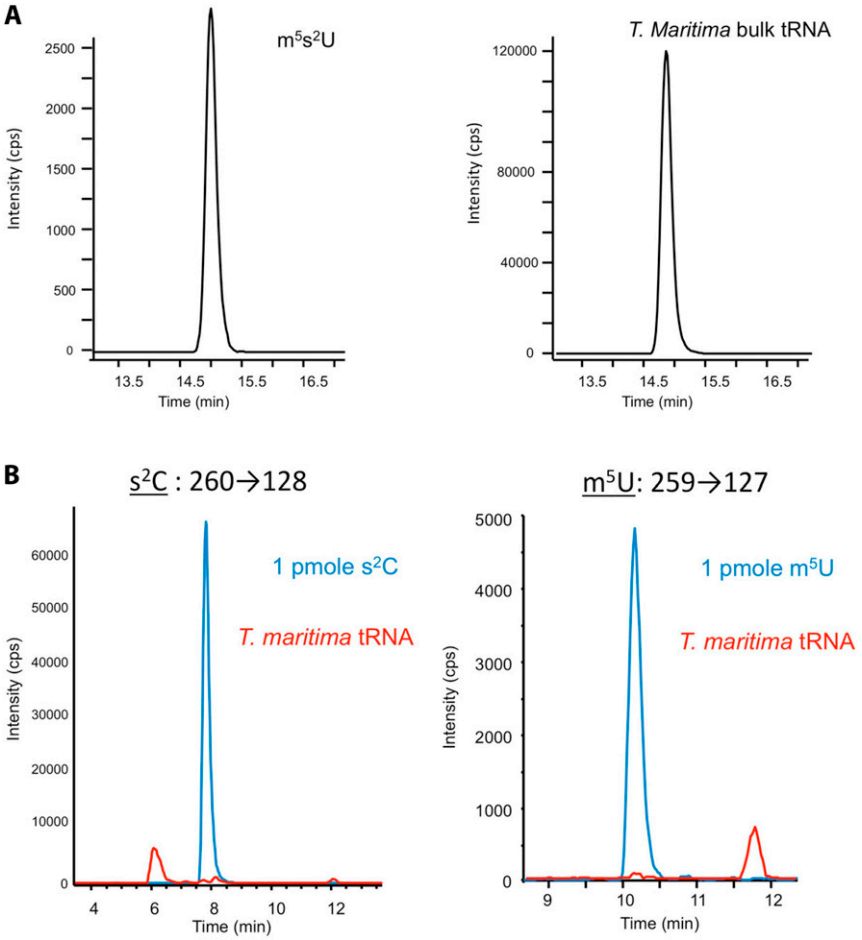

Fig. S2. Analysis of the presence of m^5s^2U, s^2C, and m^5U in tRNA within cells. (*A*) Detection of m^5s^2U in *T. maritima* bulk tRNA by HPLC on an octadecylsilyl silica gel column. (*Left*) Analysis of 1 pmol m^5s^2U standard, showing the transition *m/z* 275→143 (loss of ribose). (*Right*) Analysis of an enzymatic digest of 13 μg bulk tRNA (13.9 nmol cytosine) from *T. maritima*. (*B*) HPLC chromatograms showing the absence of both s^2C (*Left*) and m^5U (*Right*) in *T. maritima* bulk tRNA. Standards (blue) of s^2C (eluted at 8 min) and m^5U (eluted at 10.2 min), detected using transitions *m/z* 260→128 and *m/z* 259→127, respectively, were undetectable in hydrolyzed *T. maritima* bulk tRNA (red).

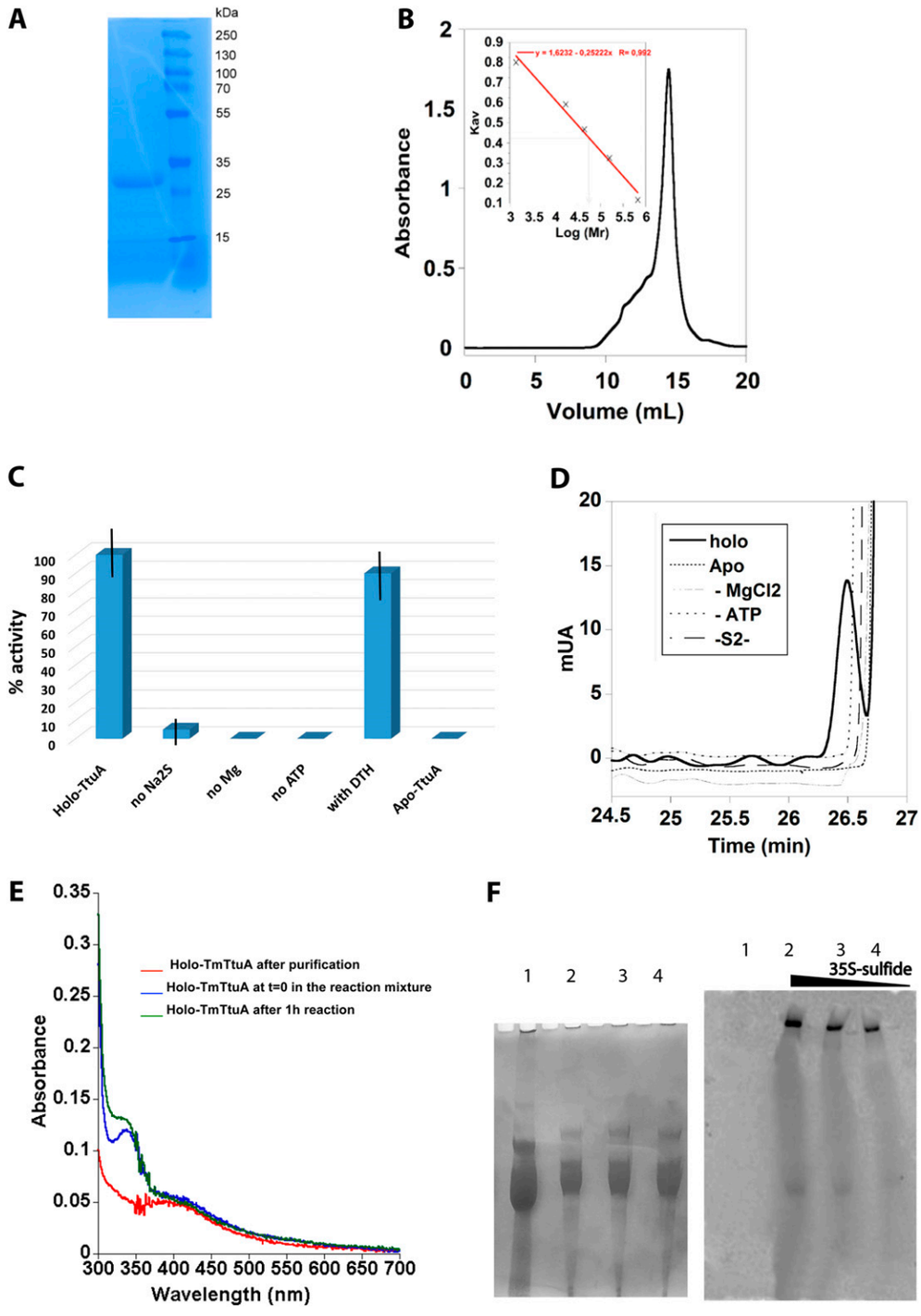

Fig. S3. Purification and activity of TmTtuA. (*A*) A 12% SDS/PAGE gel analysis of TmTtuA. (*B*) Purification of holo-TmTtuA on a Superdex 200 10/300 gel filtration column calibrated with commercial standards (BioRad no. 151–1901): Tyroglobulin (670 kDa), γ-globulin (158 kDa), Ovalbumin (44 kDa), Myoglobin (17 kDa), and Vitamin B12 (1.36 kDa). The calibration of the column (*Inset*) gave a mass of 58,277 Da for this protein, consistent with a dimeric state (theoretical mass: 69,868 Da). (*C*) tRNA thiolation control assays; 1 μM holo-TmTtuA was assayed under standard conditions (holo-TtuA); in the absence of sodium sulfide (no Na_2S), Mg^{2+} (no Mg), ATP (no ATP); or after reduction with dithionite (DTH; with DTH). Also, 10 μM apo-TmTtuA was assayed under standard conditions as control (apo-TtuA). The data shown are mean values based on three to four different experiments. (*D*) HPLC chromatograms monitoring the U54 thiolase activity of TmTtuA using *E. coli ttcA*$^-$ bulk tRNA as the substrate. After digestion of the tRNA product, the modified nucleosides were analyzed by HPLC. The data unambiguously show the absolute requirement for ATP, sulfide, $MgCl_2$, and the cluster. (*E*) UV-visible absorption spectrum of TmTtuA before and after reaction showing that the absorption band at 400 nm characteristic of the [4Fe-4S] cluster is not modified during the assay: 5 μM holo-TmTtuA (red); just after adding 5 μM *E. coli ttcA*$^-$ bulk tRNA, 500 μM ATP, 500 μM Na_2S, and 2.5 mM $MgCl_2$ (blue); and after 1 h of incubation at 65 °C (green). (*F*) Activity of TmTtuA in the presence of ^{35}S-sulfide generated by cysteine desulfurase in the presence of various quantities of [^{35}S]cysteine. After reaction, the tRNA was separated on a 7 M urea gel and analyzed by staining with toluidine blue (*Left*) and autoradiography on a Posphorimager plate (*Right*). The radioactivity present in the wells corresponds to the proteins from the incubation mixture that do not migrate in the gel. Lane 1, control (bulk tRNA alone); lane 2, 50 μCi ^{35}S-Cys; lane 3, 25 μCi ^{35}S-Cys; lane 4, 10 μCi ^{35}S-Cys.

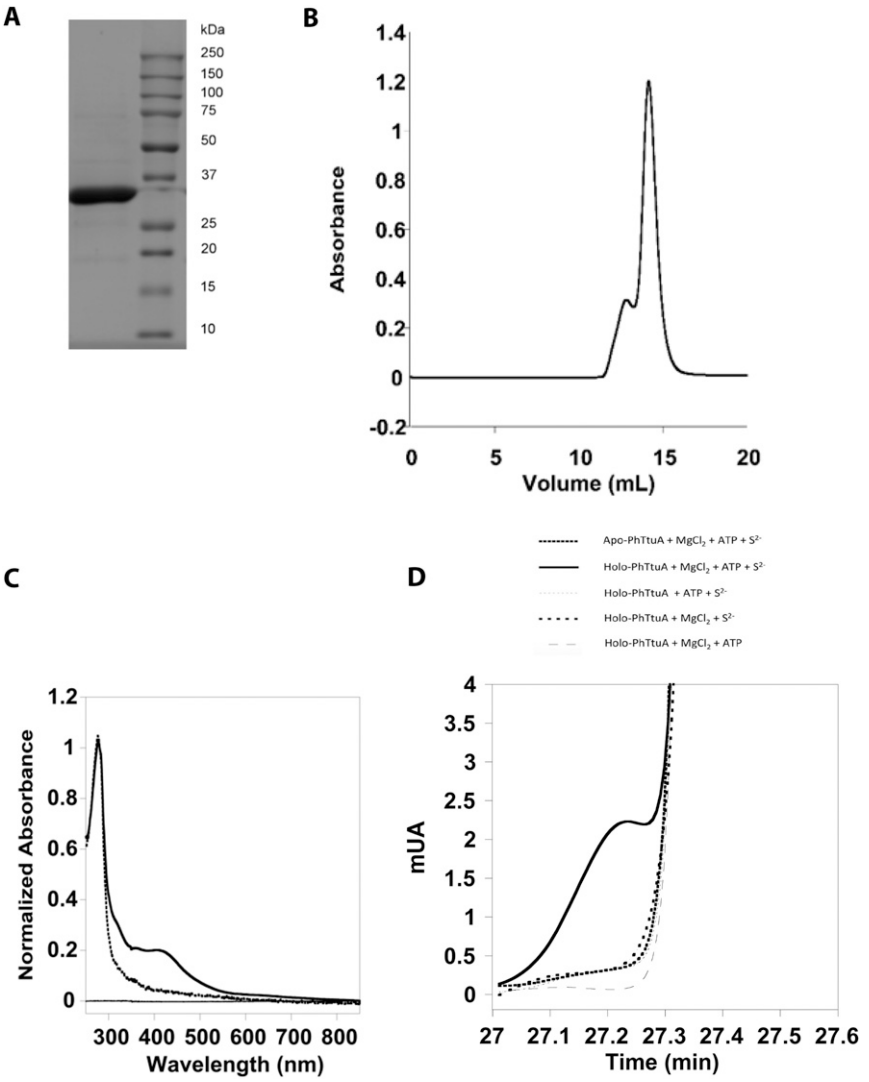

Fig. S4. Purification and activity of PhTtuA. (*A*) The 12% SDS/PAGE gel analysis of PhTtuA. (*B*) Purification of holo-PhTtuA under anaerobic conditions on a Superdex 200 10/300 gel filtration column. (*C*) UV-visible absorption spectrum of PhTtuA: dotted line, apo-PhTtuA; solid line, holo-PhTtuA. (*D*) HPLC chromatograms monitoring the U54 thiolase activity of PhTtuA using *E. coli ttcA*$^{-}$ bulk tRNA as the substrate. After digestion of the tRNA product, the modified nucleosides were analyzed by HPLC. The data unambiguously show the absolute requirement for ATP, sulfide, $MgCl_2$, and the cluster.

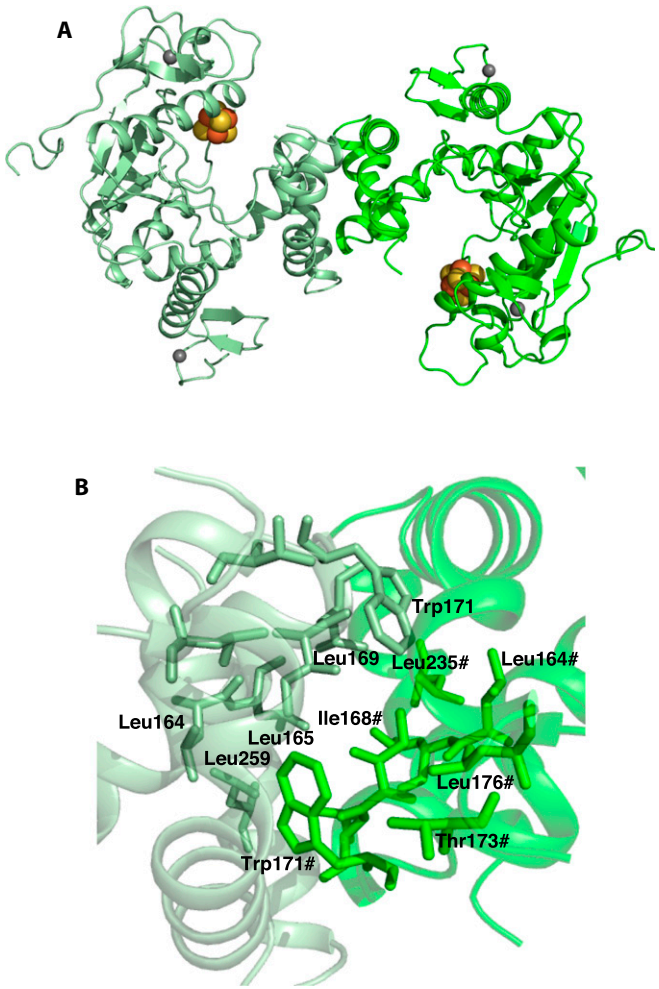

Fig. S5. Structure of the crystallographic dimer of the FeS structure. (*A*) Overall view. (*B*) Details of the interactions within the dimer. The crystallographic interface probably corresponds to the biological dimer, because the buried surface area is 4,300 $Å^2$ according to PISA (39).

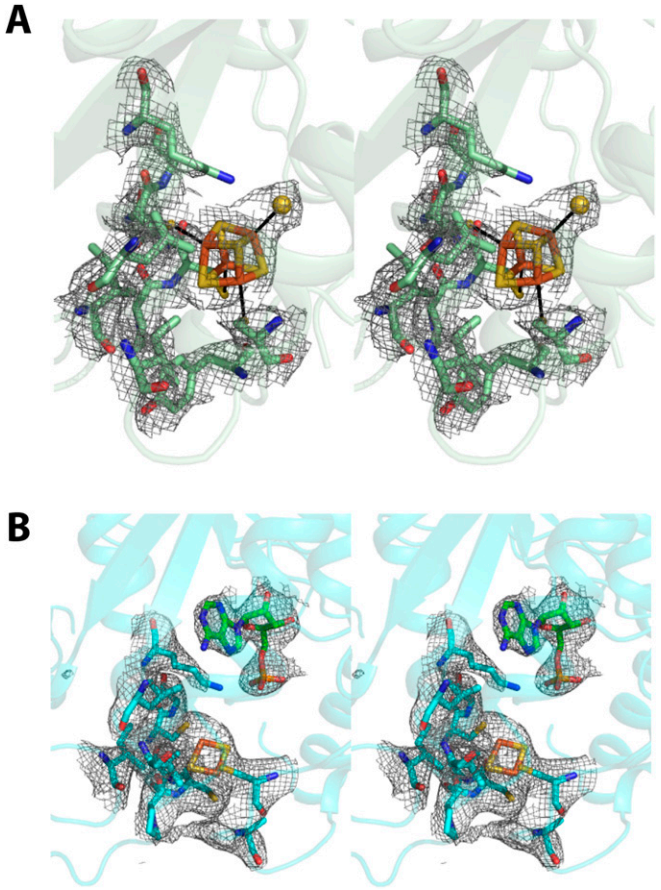

Fig. S6. Stereo views of the active site of PhTtuA. A 2Fo-Fc electron density map contoured at the level of 1σ (gray) is superimposed on the active site. (*A*) FeS structure. (*B*) AMP structure.

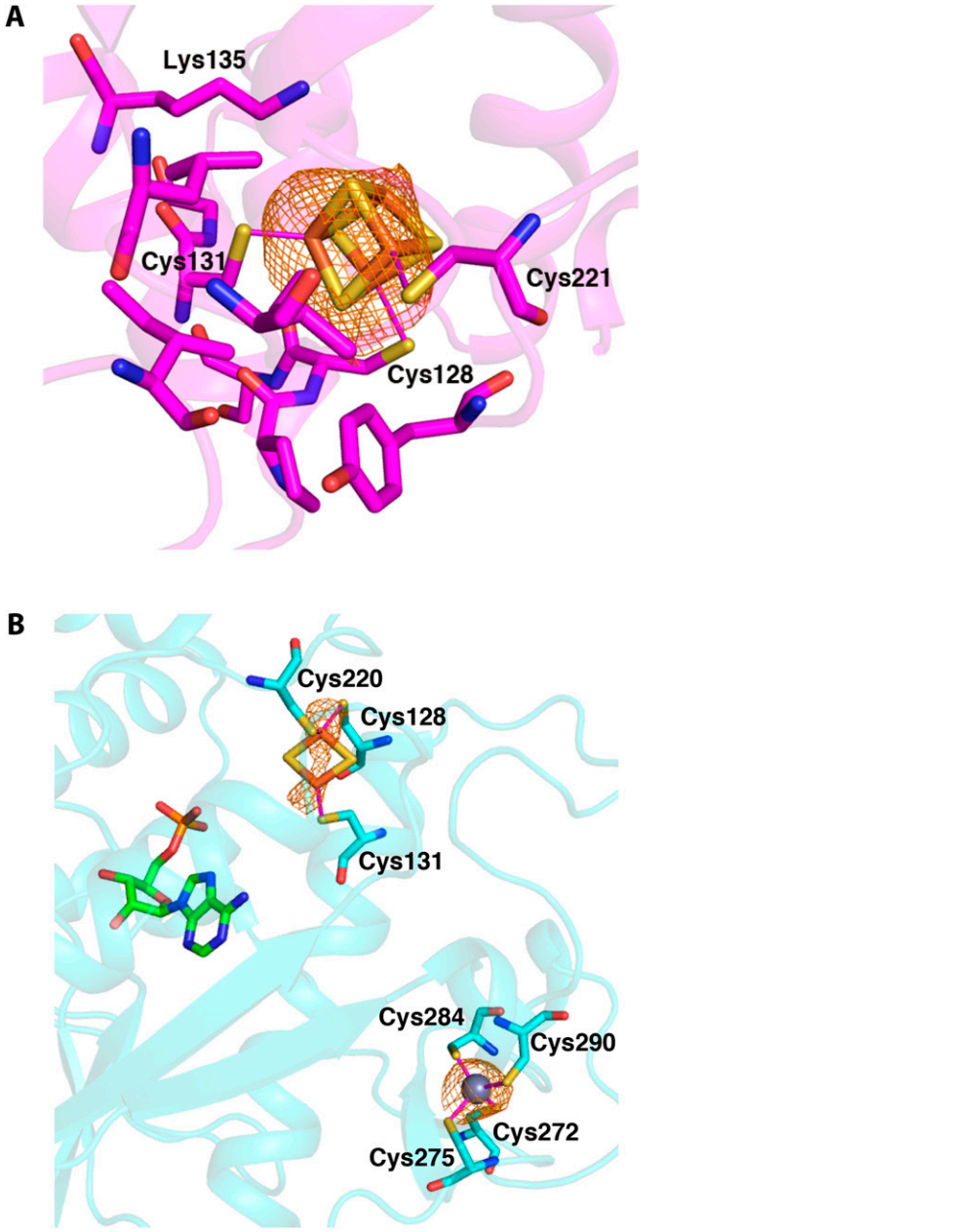

Fig. S7. Anomalous difference maps. (*A*) Anomalous difference map contoured at 3.5σ centered on the [4Fe-4S] cluster (orange) superimposed on the [Fe-S] site of molecule B of the FeS-ano structure. (*B*) Anomalous difference map calculated at the wavelength of 0.9793 Å contoured at 3σ (orange) in the region of the Zn2 zinc ion and the [2Fe-2S] cluster in molecule A of the AMP structure.

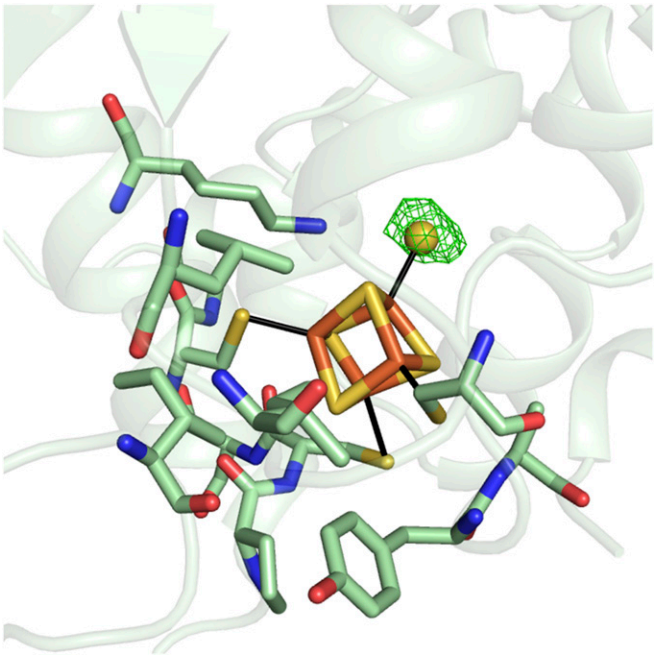

Fig. S8. Fo-Fc difference map omitting the labile hydrosulfide contoured at 2σ (green) superimposed on the [Fe-S] site of the FeS structure.

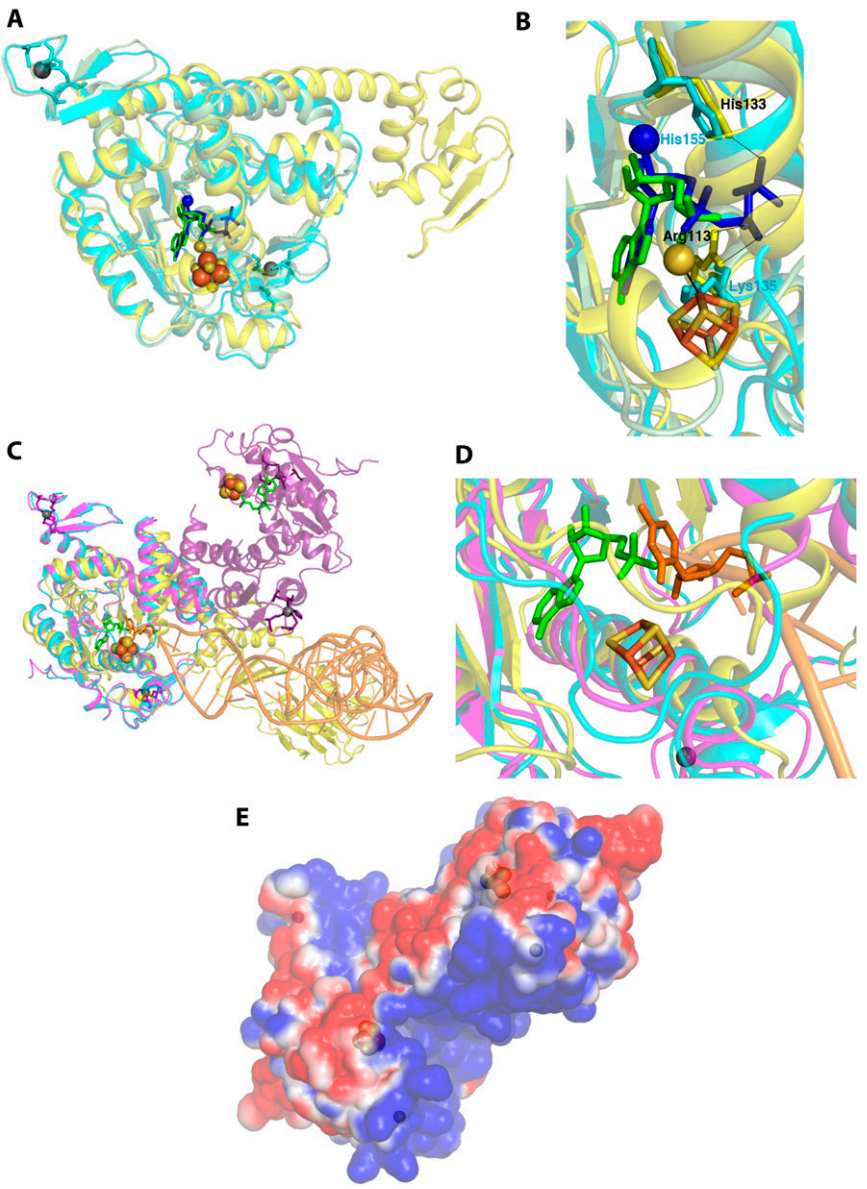

Fig. S9. Superposition of the ATP binding sites of TtuA and TilS. Residues 49–70 (corresponding to the conserved ATP binding site) from PhTtuA were superimposed onto the corresponding residues of TilS (rmsd of 0.62 Å for 22 atoms). (*A*) Monomer C of *Aquifex aeolicus* TilS (yellow) in complex with ATP and Mg^{2+} (PDB ID code 2E89) was superimposed on monomer A of the PhTtuA AMP (cyan) and the FeS structure (pale green). AMP is shown in green, the [4Fe-5S] cluster is shown as spheres, and ATP and Mg^{2+} (from TilS) are in blue. (*B*) Enlarged view of the active site showing His133 and Arg113 involved in ATP binding in TilS (shown as sticks). Zn^{2+} and Mg^{2+} are shown as gray and blue sphere, respectively. (*C*) *Geobacillus kaustophilus* TilS (yellow) in complex with tRNA (orange; PDB ID code 3A2K) was superimposed on monomers A of the PhTtuA AMP (cyan) and FeS-ano (purple) structures (rmsd of 1.60 Å for 113 atoms). The two monomers of the TtuA FeS-ano structure are shown in magenta and purple ribbons. The flipped C34 target base is represented as sticks. (*D*) Enlarged view of *C* to show the flipped cytidine 34 of tRNA bound to TilS and the PhTtuA active site pocket. (*E*) Electrostatic surface of the PhTtuA dimer (oriented as in *C*) calculated with PYMOL/APBS colored by the electrostatic potential from red (negative) to blue (positive) that shows a highly positive surface at the putative tRNA binding site.

Table S1. Data collection and refinement statistics

Crystallographic parameter	FeS (PDB ID code 5MKP)	FeS-ano (PDB ID code 5MKQ)	AMP (PDB ID code 5MKO)
Data collection			
Beamline	SOLEIL Proxima-2	SOLEIL Proxima-1	SOLEIL Proxima-1
Wavelength (Å)	0.9793	1.7389	0.9793
Space group	$P4_32_12$	$P2_12_12_1$	$P2_12_12_1$
Cell dimensions			
a, *b*, *c* (Å)	70.0, 70.0, 127.7	69.6, 72.3, 128.2	68.9, 72.3, 128.4
α, β, γ (°)	90, 90, 90	90, 90, 90	90, 90, 90
Resolution (Å)*	50–2.50 (2.65–2.50)	50–2.9 (2.98–2.9)	50–2.65 (2.72–2.65)
R_{merge}*	0.125 (2.77)	0.116 (3.09)	0.096 (4.76)
R_{pim}*	0.034 (0.876)	0.031 (0.66)	0.030 (1.44)
$I/\sigma(I)$*	16.1 (1.0)	15.1 (1.0)	13.2 (0.9)
$CC_{1/2}$*	1.00 (0.29)	0.998 (0.602)	0.986 (0.463)
Completeness (%)*	100 (99.7)	99.6 (98.8)	99.8 (99.7)
Redundancy*	14.3 (13.9)	18.6 (19.8)	12.1 (12.7)
B Wilson (Å^2)	79.8	104.1	91.9
Refinement			
Resolution (Å)	48–2.5	45–2.9	45–2.65
No. of reflections	11,624	13,036	17,292
R_{work}/R_{free}	0.1926/0.2447	0.2070/0.2445	0.2113/0.2394
No. of atoms			
Protein	2,471	4,896	4,927
Zn, Fe, S	2, 4, 5	2 × (2, 4, 4)	2 × (2, 2, 2)
AMP	—	—	46
Water	92	29	57
B factors (Å^2)			
Protein	78.5	92.3	89.5
Zn/FeS	76.7/131.9	121.2/169.1	100.7/112.8
AMP			77.6
Water	73.8	72.4	77.5
rmsds			
Bond lengths (Å)	0.09	0.08	0.08
Bond angles (°)	1.00	0.96	1.00

One crystal for each structure.
*Values in parentheses are for the highest resolution shell.